Materials Today Chemistry 36 (2024) 101936

Contents lists available at ScienceDirect

Materials Today Chemistry

journal homepage: www.journals.elsevier.com/materials-today-chemistry/

Amino acid modified graphene oxide for the simultaneous capture and electrochemical detection of glyphosate

Giulia Moro [a], Sara Khaliha [b], Angela Pintus [b], Sebastiano Mantovani [b], Matteo Feltracco [a,c], Andrea Gambaro [a,c], Tainah D. Marforio [d], Matteo Calvaresi [d], Vincenzo Palermo [b,e], Manuela Melucci [b,**], Chiara Zanardi [b,f,*]

[a] Department of Environmental Sciences, Informatics and Statistics, Ca' Foscari University of Venice, via Torino 155, 30172, Venezia, Italy
[b] Institute for Organic Synthesis and Photoreactivity, National Research Council (ISOF-CNR), via P. Gobetti 101, 40129, Bologna, Italy
[c] Institute of Polar Sciences, National Research Council (ISP-CNR), via Torino 155, 30172, Venezia, Italy
[d] Department of Chemistry 'G. Ciamician', Alma Mater Studiorum University of Bologna, via Selmi 2, 40126, Bologna, Italy
[e] Department of Industrial and Materials Science, Chalmers University of Technology, Gothenburg, S-41296, Sweden
[f] Department of Molecular Sciences and Nanosystems, Ca' Foscari University of Venice, via Torino 155, 30172, Venezia, Italy

ARTICLE INFO

Keywords:
Amino acid-functionalized materials
Graphene oxide
Electrochemical sensors
Glyphosate
Water safety

ABSTRACT

Amino acid modified graphene oxide derivatives (GO-AA) are herein proposed as active materials for the capture and consequent electrochemical detection of organic pollutants in aqueous media. Glyphosate (GLY), an herbicide present in many water compartments, was chosen as benchmark species to test the effectiveness of these materials for its electroactive nature, allowing direct evidence of the capture event. L-Lysine, L-Arginine or L-Methionine were grafted on GO surface through epoxide ring opening reaction, promoting the amino acids binding and the concomitant partial reduction of GO. The synthetic process results in a charge resistance drop from 8.1 KΩ for GO to 0.8–2.1 KΩ for the various GO-AA, supporting the applicability of these materials in electrochemical sensing. The resulting GO-Lysine, GO-Arginine and GO-Methionine were exploited for GLY adsorption from water. GO-Lysine was found to have the strongest interaction with GLY, with a removal efficiency of 76 % after 1 h, which is about two-fold higher than those of granular activated carbon, the industrial benchmark adsorbent. GO-AAs outperform the pristine unmodified material also when exploited as active materials for the capturing and following electrochemical detection of GLY. GO-Lysine showed the best sensitivity and allowed the recognition of GLY in water even when present at concentration levels down to 2 μg/L. Molecular dynamics simulations confirmed that the enhanced performance of this material can be ascribed to the hydrogen bond and salt bridge interactions between Lys moieties and GLY, originated from hydrogen bond and salt bridge interactions.

1. Introduction

Safe water supplies are essential to environmental protection, animal and human health, quality of life, economic growth and sustainable development [1,2]. Assuring water safety is considered a global priority [3,4] highlighted in the Agenda 2030 of the United Nation as Sustainable Development Goal 6 [5]. Indeed, the healthiness of the hydric compartment is threatened by the continuous release of toxic substances, including pharmaceuticals, microplastics, plasticizers, pesticides, and metals ions due to anthropogenic actions [6]. Among these chemicals, the ones listed as contaminants of Emerging Concern (ECs) [2,7] are rising the interest of environmental agencies: their ecological/toxicological impacts are still under evaluation and their level in water needs to be constantly monitored [8]. In this context, analytical tools to assess the presence of these pollutants in water are urgently required to map, prevent and, eventually, reduce chemical and risks especially linked to drinking water consumptions [9–11]. At present, quantification of ECs in drinking water is performed mainly by chromatographic techniques since they are characterized by very low detection limits [12]. However, they are time-consuming, expensive and

* Corresponding author. Department of Molecular Sciences and Nanosystems, Ca' Foscari University of Venice, via Torino 155, 30172, Venezia, Italy.
** Corresponding author.
E-mail addresses: manuela.melucci@isof.cnr.it (M. Melucci), chiara.zanardi@unive.it (C. Zanardi).

https://doi.org/10.1016/j.mtchem.2024.101936
Received 14 November 2023; Received in revised form 8 January 2024; Accepted 21 January 2024

can only guarantee very punctual monitoring of chemical parameters since analysis has to be carried out after a proper sampling procedure. Therefore, many contaminants can be accidently introduced in distribution line due to the lack of suitable analytical tools and of frequent, large-scale monitoring plans. In this scenario, the integration of sensor systems in the water distribution networks rapresent a possible way to overcome these limitations and improve water monitoring strategies [13].

Electrochemical sensors are commonly used for the detection of chemical parameters in liquid samples since consisting of miniaturized, portable, and user-friendly devices [14,15]. Their analytical performance can be widely modulated by accurate choice of the sensing element and of the electrochemical parameters used for the detection of the target analyte. A selective response can be achieved using voltammetric techniques especially when the analyte is an electroactive species that are oxidized/reduced at a well-defined electrochemical potential [16]. The sensing element further contributes to improve the selectivity, the sensitivity and the limit of detection of the final platform. Among various materials proposed to such a purpose, graphene derivatives have emerged as valuable active elements of electrochemical sensors [17–19]. The main advantages in the use of these materials lay in their large surface-to-volume ratio, that allows a high number of active sites to be in contact with the solution [20] and to the possibility of tailoring the functionalization of the carbon nanosheets to include (bio)receptors capable to induce selective interaction with the target [21–23].

For similar reasons, graphene derivatives were also applied to the purification of water from several organic and inorganic contaminants. Thanks to the numerous oxygen-containing functional groups present on the surface of the nanosheets, the contaminants are adsorbed at the surface of these materials [24,25]. These adsoprtion processes can be further enhanced by functionalizaing the nanosheets with suitable organic moieties [26–29]. The early detection of organic contaminants in water requires the use of sensing materials capable to efficiently interact, i.e. capture, the target and to transduce the recognition event in a well measurable signal (Fig. 1). Therefore, we propose the use of graphene-based materials for the development of electrochemical sensors to be applied in the water monitoring of organic pollutants. Due to their proved adsorption capability toward several organic contaminants [28,29], we selected the use of amino acids-modified graphene oxide (GO-AAs) for such application. Amino acids (AAs) are natural, cheap building blocks with a wide chemical variability. Their covalent grafting on graphene oxide (GO) can be achieved under mild reaction conditions, allowing to tune the surface chemistry of the nanosheets with minor effect on their processability. Recent studies showed that the AA moieties create preferential capturing sites on the basal plane of graphene, leading to enhanced interaction between the nanosheets and targeted molecules, allowing their applications as sorbent of emerging contaminants in water [30,31]. The adsorption selectivity is strongly related to the chemical structure of the AAs, due to the balance between the contribute of electrostatic, hydrophobic and van der Waals interactions between AAs and GO nanosheet surface promoted by the AAs exposed moieties.

As a case of study, we targeted the detection of glyphosate (N-[phosphonomethyl]glycine, GLY), that is a widely used organophosphate herbicide commercialized by Monsanto since 1974 under the name RoundUp. Over the yars it has been massively used in agriculture to treat crops, especially maize, soybean and cotton [32–34]. Despite its toxicity, GLY is considered to have a lower environmental impact compared to other water contaminants [35]. The intensive use of GLY has generated an increase in its concentrations in water and soil [36–39] with harmful effects on our ecosystem and on human health [40,41]. This forced the authorities to indicate GLY as one of the emerging contaminants which requires to be strictly monitored in the environment [42]. Due to the advantages previously described in the use of sensors for such a purpose, many devices have been proposed so far for the detection of GLY in environmental matrices [43,44]. However, most of these sensors, especially the ones based on the enzymatic inhibition mechanisms [45–47], are not applicable to the continuous monitoring of GLY in the water distribution network.

Beside these ecological reasons, the choice GLY as a target to prove the effectiveness of the approach proposed is motivated by the electroactive nature of this species, which can undergo an oxidation process at carbon-based surfaces according to a mechanism previously proposed (Fig. S1 of the ESI) [48,49]. This implies that the performance of tailored

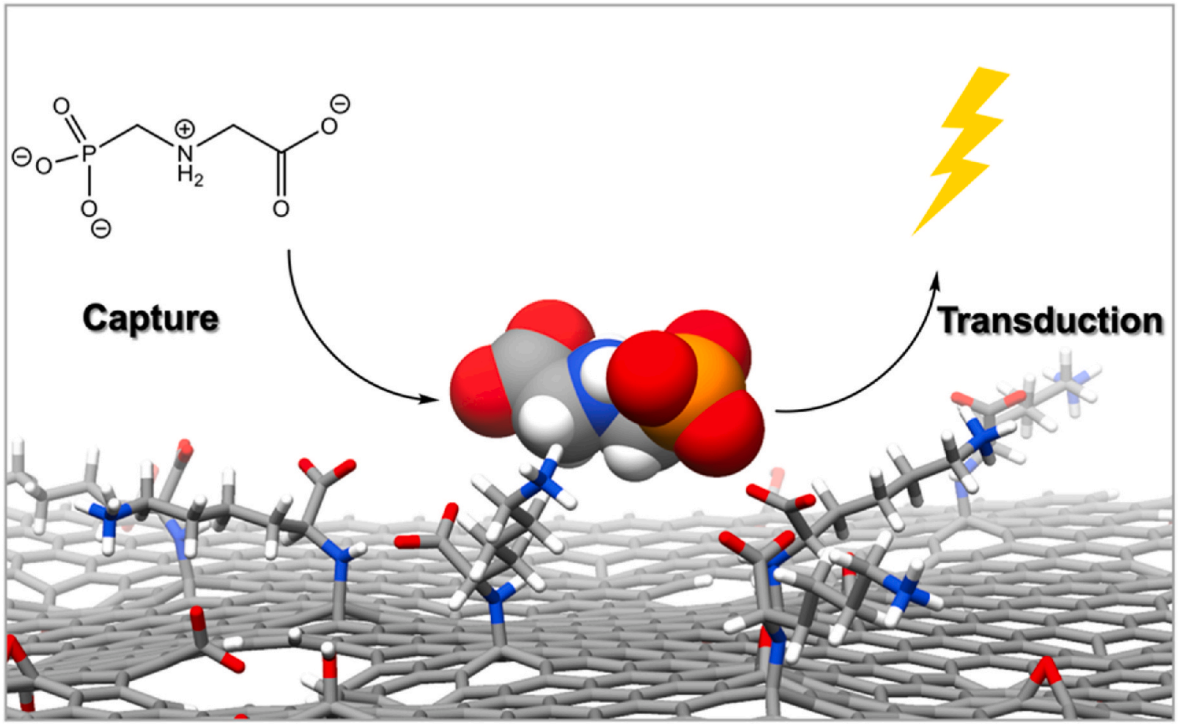

Fig. 1. Schematic representation of the double role of GO-Lys: adsorption, i.e. pre-concentration, and following electrochemical detection of GLY.

materials for GLY capturing and detection can be easily compared by simply collecting the voltammetric response deriving from the direct GLY oxidation. Due to the electroactive nature of this species, Santos et al. recently highlighted the advantages in the use of graphite oxide carbon paste electrodes for the rapid detection of GLY from groundwater samples by a simple and inexpensive electrochemical device [49]. These results encouraged us in exploiting functionalized graphene derivatives to take advantage of their dual-activity in capturing (i.e., pre-concentrating) and then detecting GLY. On the basis of our previous experience, various GO-AA are here proposed and tested as active layers of these electrochemical sensors, namely GO-Lysine (GO-Lys), GO-Arginine (GO-Arg), and GO-Methionine (GO-Met). The rationale behind the choice of these AAs is that they have similar alkyl chain size but different surface charge (Met is neutral while Lys and Arg are charged positively at pH 7) and binding capability. On one side, the positively charged L-Lysine and L-Arginine were chosen to promote the electrostatic interactions with GLY, which bears a negative charge at neural pH, stabilizing the analyte interaction with the electrode surface. On the other side, the highly hydrophobic L-Methionine was selected to improve the van der Waals/hydrophobic interactions with the target and enhance its affinity for the modified surface.

2. Materials and methods

2.1. Reagents

GO and reduced graphene oxide with 80 % of carbon atoms (rGO) were purchased from Layer One (S-126/36) and used without further purification. L-Methionine methyl ester (Met), L-Lysine (Lys), L-Arginine (Arg), potassium hexacyanoferrate(III), potassium hexacyanoferrate(II) trihydrate, and ferrocenemethanol (Fc) were purchased from Sigma-Aldrich and used without any further purification. Plasmart 100 microfiltration modules (Versatile™ PES hollow fibres, cut off 150 nm, filtering surface 0.1 m^2, pore size 100–200 nm) for GO-AA purification were provided by Medica S.p.A (Medolla, Italy). Granular Activated Carbon (GAC) was purchased from CABOT Norit Spa (Ravenna, Italy, Norit GAC 830 AF, MB index min 240 mg/g, BET surface area >1000 m^2/g); to remove sub-millimetric particles GAC was washed with deionized water at a mild flux, then dried overnight in an oven at 40 °C.

All solutions were prepared with deionized water (18.2 MΩ×cm resistivity). GLY (N-phosphonomethyl glycine, 99.2 % w/w) was acquired from Sigma-Aldrich, whereas the isotopically labelled internal standard used for chromatographic tests, namely glyphosate-2-13C, 15 N, were purchased form Merck KgaA (Darmstadt, Germany). Britton-Robinson (BR) buffer, used for electrochemical tests, was prepared from H_3PO_4, H_3BO_3, CH_3COOH and NaOH, all acquired from Sigma-Aldrich.

2.2. Synthesis of GO-AA and characterization

GO-AA were prepared by epoxide ring opening reaction at pH 9 [28, 50]. The synthesis of GO-Met and GO-Lys has been previously described, while GO-Arg is herein prepared for the first time (in a previous work it was prepared at pH 13). L-Arg (34.4 mmol, 6 g) solution in MilliQ water (50 mL) was added to 400 mL of GO suspension (5 mg/mL, MilliQ water, sonicated for 2 h). The mixture was kept under stirring at 80 °C for 24 h, then 5 mL of EtOH were added. The crude product was purified by microfiltration on commercial VersatileTM PES module (Plasmart 100, Medica SpA) in loop filtration mode by using a peristaltic pump at 100 mL/min. Pure water was progressively added to the feed solution (tot. volume = 3.2 L) [27]. The process was stopped when a neutral pH was measured in the permeated water. 2.3 g of GO-Arg were obtained after freeze drying. The Arg loading was determined by Elemental Analysis (EA) (Unicube Elemental analyzer).

2.3. Adsorption and kinetic test on GLY

A standard solution of GLY at 250 mg/L was prepared dissolving 4.5 mg in 18 mL of milliQ water. It was then diluted till reaching the concentration of 0.5 mg/L, then stored at 4 °C.

25 mg of GO, GO-AA or rGO were sonicated in 2.5 mL of MilliQ water for 2 h, then 22.5 mL of tap water were added (total volume = 25 mL, pH 6.9). Analogous tests were repeated with suspensions spiked with 100 mL of the GLY stock at 0.5 mg/L, to reach the final concentration of 2 mg/L. GAC experiments were performed under the same conditions but without previous sonication. Samples were then left under rotary stirring and tested after either 15 min or 1h contact times. Three replicates of each condition were carried out. The supernatant was collected for centrifugation at 10.000 rpm for 10 min.

2.4. HPAEC-MS/MS analysis

The residual concentration of GLY in tap water after treatment with GO derivatives was defined by applying a chromatographic method previously developed [39], using glyphosate-2-13C,15 N as internal standards. A high-pressure anion exchange chromatograph (HPAEC) (Dionex™, Thermo Scientific™, ICS-5000, Waltham, USA) was coupled to a TSQ Altis™ Plus Triple Quadrupole Mass Spectrometer (Thermo Scientific™, ICS-5000, Waltham, USA). Chromatographic separation was performed using an anion exchange column Dionex IonPac™ AS19 RFIC™ 2 × 250 mm (Thermo Scientific™) equipped with a guard column Dionex IonPac™ AG19 RFIC™ 2 × 50 mm (Thermo Scientific™). Results were corrected using the instrumental response factor by analysing a solution with a mean concentration of 5 μg/L.

2.5. Preparation of GO-AA modified electrodes

The performance of GO-AA in acting as adsorbent and electroactive material for GLY detection was tested by depositing a thin coating of materials on graphite disk electrodes (GEs – 5 mm diameter). Prior to be modified, GEs were polished with a 1.0, 0.3 and a 0.05 mm water-based γ-alumina slurry on microcloth pads, sonicated in MilliQ water for 2 min, rinsed with water and dried. Homogenous suspensions of GO-AA were obtained by sonicating (60 kHz) 0.5 mg of each GO-functionalized powder in 1 mL deionized water. The drop casting of GO-based materials (GO-Lys, GO-Arg, GO-Met and GO) was operated following a two-steps protocol. Firstly, GE surfaces were covered with 4 μL of GO-Lys/GO-Arg/GO-Met/GO suspensions; then, once the aqueous solvent was evaporated, a second deposition of 4 μL of the same suspensions was carried out. The GO coating was further treated by polarizing the electrode for 300 s at a fixed potential of −1.25 V in 0.1 M phosphate buffer solution pH 7.4, to reduce the GO to rGO. Before the analysis, the modified electrodes were dipped in 0.5 M $LiClO_4$ aqueous solution for 10 min and rinsed with deionized water [43].

2.6. Electrochemical tests of GO-AA

Electrochemical measurements were carried out at room temperature (20 °C) using a computerized Autolab PGSTAT 12 (Ecochemie, Utrecht, The Netherlands) controlled with NOVA 2.1 software. All experiments were performed with a conventional three-electrode single-compartment glass electrochemical cell (V_{cell} = 10 mL) equipped with modified GE as working electrodes, Ag/AgCl sat. KCl, as reference electrode, and a platinum wire, as counter electrode. All voltammograms report the current density calculated considering the use of GE possessing a geometric area of 0.20 cm^2.

All modified GE were characterized by cyclic voltammetry (CV) in the potential window between −0.2 and + 0.6 V, at various scan rates (20, 50, 100, 150, 200 mV s^{-1}) in 0.5 M $LiClO_4$ aqueous solution in absence and in presence of 1 mM Fc. In order to confirm CV data, electrochemical impedance spectroscopy (EIS) analysis was performed

in a 5 mM of $[Fe(CN)_6]^{3-/4-}$, 0.5 M $LiClO_4$ solution: the electrode was polarized at the open circuit potential (OCP) by applying an *ac* perturbation of 5 mV with a frequency ranging between 0.1 Hz and 10 KHz. This electrolyte was preferred for these preliminary tests aimed at studying the charge transfer resistance of the materials in analogy to what reported in previous works [51,52].

All solutions containing GLY were freshly prepared and stored at 4 °C until tested. Preliminary voltammetric traces, aimed at verifying the most suitable conditions to acquire the signal due to GLY oxidation, where performed in BR buffer solutions at pH 5, 6, 7 and 8, in absence and in presence of 20 mg/L GLY.

The capture and transduction capability of the GO derivatives for GLY was tested by depositing a drop of the analyte solution directly on the modified electrodes surface. We used GLY concentration of either 10 mg/L, for initial tests, or much lower, 2 mg/L, closer to that expected in contaminated tap water. We studied the kinetics of GLY adsorption on the samples using various incubation times (15 min, 1h, 4h, 18h) and then recording the signal deriving from GLY oxidation in a 0.2 M BR solution at pH 6 [49]. After GLY incubation, the modified GEs were rinsed with abundant water to record only GLY molecules adsorbed on the coating. The electrochemical signal was recorded by Differential Pulse Voltammetry (DPV), by scanning the potential between 0.6 and 1.6 V, by adopting the following parameters: 70 mV as the pulse amplitude, 0.5 s as the modulation time, 10 mV as the step potential and 20 mVs^{-1} as the scan rate. These parameters were chosen at the end of some preliminary tests by observing the effect of each parameter at time, as a compromise between the peak intensity (i.e., the faradaic current affecting the sensitivity), and the residual capacitive current.

In a second step, to achieve conditions closer to the real frame, GO-Lys was further tested by simply dipping the electrode in the standard solution of GLY at concentration ranging from 2 to 100 μg/L. The different solutions were first tested by progressively increasing the concentration of GLY and, then, in a random sequence, to avoid possible artifacts due to memory effects which can derive from the interaction of GLY with the material. The electrochemical signal was collected by DPV, by adopting the same parameters previously described.

The samples of tap water spiked with known concentrations of GLY were freshly prepared. To assure the buffering capability and to increase the ionic strength of the samples, a mixture of boric, phosphoric, and acetic acids was added to the final, equimolar, concentration of 0.4 M. Prior to proceeding with the DPV measurements, the pH of each sample was measured and adjusted to pH 6 (if needed) by adding a few drops of 1 M sodium hydroxide or acetic acid solution. The samples were then analyzed as described above.

2.7. Molecular dynamics simulations

GO-Lys, GO-Arg, GO-Met and rGO were parametrized using the GAFF force field [53]. A well-defined number of epoxy, hydroxyl, carbonyl, carboxylic acids, Lys, Arg, and Met groups were positioned on the graphene sheet to reproduce the experimental XPS data [29]. The GAFF force field [53] was also used to parametrize GLY. The atomic charges of GLY were obtained by using the Restrained Electrostatic Potential (RESP) method [54]. The GLY/rGO and GLY/GO-AA systems were neutralized by adding counterions and placed in a box of TIP3P water molecules. The systems were minimized, equilibrated and then 100 ns of MD simulations were carried, using AMBER 16. The binding affinities of GLY to rGO and to GO-AA were calculated by using the Molecular Mechanics-Generalized Born Surface Area (MM-GBSA) model [55].

3. Results

3.1. Synthesis

The three different GO-AA tested (Fig. 2) were synthetized by epoxide ring opening reaction and then purified by microfiltration (details in section 2.2). The amino acids loadings were 16 % (GO-Arg), 15 % (GO-Lys) and 6 % (GO-Met) with partial reduction (about 20 %) of the carbon nanosheets (e.g. O/C = 0.77 and 0.59 for GO and GO-Arg, respectively). The low O/C ratio is particularly important when considering the final use of these materials in electrochemical sensing: thanks to the partial reduction deriving from the synthetic procedure, the materials may be directly used for the electrochemical transduction without any further pre-treatment. Conversely, the charge transfer resistance of pristine GO is so high that a chemical or an electrochemical reduction is required [51]. For this reason, we then compared the performance of GO-AA, both for adsorption and for sensing purposes, with a highly conductive rGO sample featuring a O/C ratio of 0.25, either commercially available (see Par. 3.2) or obtained by electrochemical reduction of pure GO at −1.25 V (see Par. 3.4) [51].

3.2. Adsorption capability of GO-AA

Adsorption kinetic studies were carried out comparing GO-AA samples with three benchmark materials: pure GO, pure rGO, and GAC, widely used as industrial sorbent. The experiments were carried out in triplicate using a fixed concentration of GLY (2 mg/L). Fig. 3 shows the % of GLY removal for all samples, at different contact times, namely 15 min and 1h.

For short contact time (15 min) rGO showed the highest removal (60 %), while all the GO-AA showed lower adsorption performance with removal of 10 % (GO-Met), 22 % (GO-Arg), and 29 % (GO-Lys) respectively. GAC and GO showed comparable adsorption capacity of about 25 % and 20 %, respectively. After 1h contact time the adsorption capacity for all the materials increased, reaching 77 % for GO-Lys and 70 % for both GO-Arg and rGO, while a much lower value was found for GO-Met (38 %). This behavior is consistent with the chemical nature of these AA, since both Lys and Arg possess basic amino acid residues, so that they both show a positive net charge ($pK_{Lys} \approx 10.5$ and $pK_{Arg} \approx 12.5$) at pH values close to neutrality, which are typical of tap water. Since GLY has a net negative charge at these pH values ($pK_{a,3} = 5.6$), the

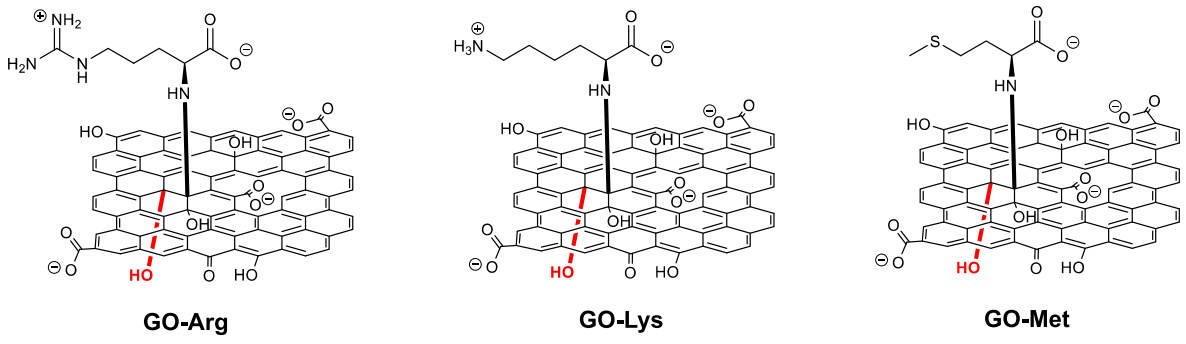

Fig. 2. Chemical structure of GO-AA used in this work.

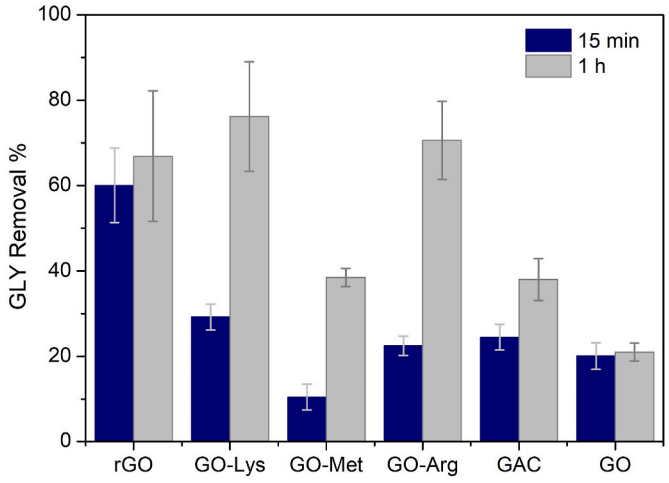

Fig. 3. Removal % of GLY at different contact time (15 min, 1h) on the different materials tested: rGO, GO-Lys, GO-Met, GO-Arg, GAC and GO. Total volume = 25 mL, sorbent amount = 25 mg, $C_{In,GLY}$ = 2 mg/L. The bars report the standard deviation calculated from triplicate measurements.

presence of positively charged primary amino groups could explain the enhanced adsorption observed for GO-Arg and GO-Lys. All GO-AA materials showed higher removal capability than GAC (20 %), highlighting the potential of such materials for water remediation from GLY.

3.3. Electrochemical characterization of GO-AA

The possible application of GO-AA in electrochemical sensing was preliminary tested by voltammetric responses recorded in absence and in presence of a benchmark electroactive species. The behaviour of the functionalized materials was compared with that of rGO, obtained by an electrochemical pre-treatment of GO at −1.25 V to partially restore the sp^2-hybridized carbon network [51,56];as already stated, this process in mandatory to make the conductivity of the material suitable for the application in the electrochemical frame. Conversely, the GO-AA samples could be used with no reduction pre-treatment. The volume of all the GO-based dispersions was fixed at 8 μL, to normalize the behaviour of the various materials in respect to the mass deposited. We obtained in all samples, a repeatable response, not affected by ohmic resistance, recording CV responses in the pure electrolyte solution (see Fig. S2). The values of the current recorded at +0.2 V are linearly dependent from the scan rate (Fig. 4a), as expected for purely capacitive current induced by the presence of a conductive material. CV responses also showed that GO-Lys and GO-Arg coatings has lower capacitive contributions compared to rGO and GO-Met. Also, this difference ascribed to the benefic effect of the positive chargers induced by the AA residues, balancing the intrinsic negative potential of GO. GO-Met showed capacitive contribution halfway between the ones of rGO and GO-Arg/GO-Lys, as expected for a material bearing neutral moieties at the electrode solution interface, that can shield the negative charged on rGO nanosheets.

Responses in the pure electrolyte solution evidence the good conductivity of all GO-AA derivatives, in agreement to what previously observed for other graphene-based materials and to the O/C ratios previously discussed [57].

This conclusion can be better supported by testing the resistance to charge transfer in presence of a redox probe undergoing a reversible electrochemical process, namely Fc. This probe was specifically selected since it does not induce any electrostatic interaction with the surface and undergoes an outer-sphere charge transfer mechanism, i.e., an electrochemical process not implying direct contact with the surface. In all samples, the peak-to-peak separation between the anodic and cathodic responses (ΔE) was about 59 mV (Figs. S3 and S4), confirming that the presence of these electrode modifiers does not affect the Nernstian behaviour of Fc redox process with respect to the bare, well conductive, underlying GE. A linear dependence of the anodic peak current with respect to the square root of the scan rate was obtained for each modified electrode (see Fig. S5), as expected for a mass diffusion-controlled process occurring at an electrochemical surface characterized by a low charge transfer resistance.

This behaviour indicates that the intensity of the current peak (i_p) can be expressed by the Randles-Sevcik equation:

$$i_p = \left(2.69 \times 10^5\right) n^{3/2} A D^{1/2} C^b v^{1/2}$$

where n is the number of electrons exchanged, A is the electroactive area (which is often different from the geometric one especially for modified electrodes), D is the diffusion coefficient of the electroactive species which is present in the bulk of the solution at the concentration C^b, and v is the potential scan rate. From the slope of the plots reported in Fig. S5, it was possible to evaluate the electroactive area of the different GO-AA modified electrodes in respect to the rGO ones. The normalized electroactive surfaces (Fig. 4b) highlight that the use of functionalized materials does not imply any significant increase of the active area because of the chemical functionalization of the nanosheets, meaning that the possible higher sensitivity observed for GLY oxidation at these electrode

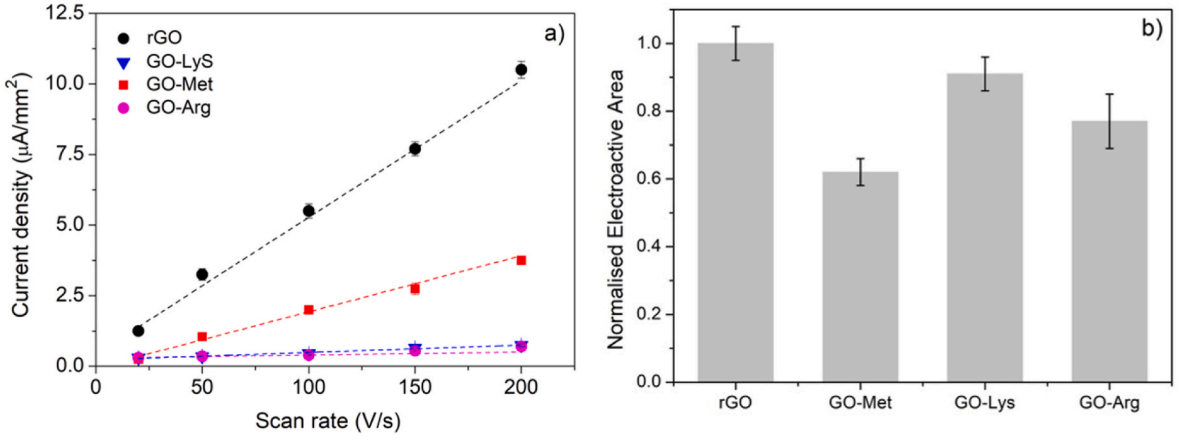

Fig. 4. a) Plot of the capacitive current densities recorded at +0.2 V *vs* the scan rate for the different materials tested; the values were obtained from CV responses recorded in 0.5 M $LiClO_4$ (see Fig. S2). **b)** Normalized electroactive surface of GO-AA in comparison to rGO; the values are obtained according with the Randles-Sevcik equation, from the slope of plots in Fig. S5 recorded for the different material with respect to rGO, whereas the relative error was calculated out from triplicate measurements.

coatings cannot be ascribed to the higher surface.

Finally, to better highlight the variation in the charge transfer resistance (R_{ct}) of GO after the chemical functionalization, we did EIS tests in a $[Fe(CN)_6]^{3-/4-}$ solution. As observed from the Nyquist and the Bode plots (see Fig. S6), the materials showed different interfacial properties. The Nyquist plots were fitted by a simple electrochemical equivalent circuit characterized by two resistors, describing the contribution of the solution resistance (R_s) and of the charge transfer resistance at the electrode/solution interface (R_{ct}), a constant phase element (CPE) and a Warburg element (W). The data analysis confirmed that R_{ct} significantly decreases from 8.1 KΩ of GO to 0.8–2.1 KΩ for all GO-AAs highlighting the applicability of these materials in the electrochemical frame.

3.4. Performance of GO-AA for GLY capture and detection

The capability of graphene derivatives to detect GLY by an electrochemical approach was preliminary evaluated by a GO-Lys modified electrode in a solution containing a fairly high concentration of contaminant, namely 20 mg/L. Fig. 5a reports the CV responses obtained in absence and in presence of GLY, clearly evidencing an anodic process centred at about +1.35V. We performed these experiments at a pH 6 in analogy to previous reports concerning the detection of this species [48,49] and claiming that this condition allows the presence of the molecule in the double deprotonated form, which is considered the electroactive one (see Fig. S1 in Supporting Information). Indeed, we could preliminarily verify that higher sensitivity can be obtained at this pH value (see Fig. S7 in SI), since heavy oxidation of the underlying electrode surface occurs in solutions at lower pH at the potentials which are required for GLY oxidation, whereas partial deprotonation of the Lys moieties may affect the interaction between GO-Lys and the negatively charged pollutant when using more alkaline solutions.

Since the sensitivity of linear sweep voltammetric techniques is normally too low to allow the detection of slight number of contaminants present in water, we moved to a pulsed voltammetric technique, namely DPV, to increase the signal-to-noise ratio. The electrochemical signals recorded in absence and in presence of 20 mg/L GLY (Fig. 5b), still showed an evident peak centred at +1.35 V. To better highlight the contribution of the GLY oxidation in the voltammetric signal, we report in the inset the signal subtracted for the relevant blank.

Once defined the capability of GO derivatives to achieve an electrochemical signal due to the presence of GLY in solution, we tested the application these coatings to seize and, subsequently, to detect GLY in aqueous matrices. For these preliminary tests, a 10 mg/L GLY aqueous solution was used. After the capturing step, the electrode was abundantly rinsed with deionized water aiming at removing weakly adsorbed GLY traces and at estimating only the fraction that was stably captured by the material. The evaluation of the different capturing capability of the various materials was carried out by comparing the DPV signals obtained in similar conditions after subtraction of the relevant blank signal (see Fig. 6a). As observed, the adsorption of GLY at all graphene-based coating was confirmed by recording an oxidation peak centred at about +1.35V.

Similar experiments were repeated in solutions of GLY at a concentration much closer to that expected in contaminated tap water, i.e. 2 μg/L. Fig. 6b shows the average current values obtained for three experiments performed with the same experimental conditions, together with the relevant standard deviation. As observed, only GO-AAs allow the detection of GLY at this particularly low concentration after 15 min of contact time, indicating the effectiveness of the amino acid in capturing the contaminant present in the water solution. Among them, GO-Lys showed the highest pre-concentration efficiency and reproducibility, as testified by a small relative standard deviation (RSD) of 9 % in comparison to 40 and 35 % obtained for GO-Met and GO-Arg, respectively. As previously discussed, the higher sensitivity observed for GO derivatives with respect to the pristine material cannot be ascribed to an increment of the electroactive area on passing from pristine to functionalized materials, as stated on looking Fig. 4b.

To confirm that GO-Lys can outperform pristine rGO for GLY detection, the previous experiment in a GLY solution with a concentration of 2 μg/L was extended to longer contact times. Fig. 7 shows that at any time the voltammetric signal obtained after pre-concentrating GLY on the functionalized material is higher than that recorded at rGO. GO-Lys reached a sensitivity that, at the equilibrium conditions, is three times higher than the one obtained at the pristine material. The more marked capturing efficiency of GO-Lys observed here with respect to adsorption tests previously discussed (Fig. 3) can be ascribable to the different experimental configuration of the two tests: the presence of Lys residues on graphene nanosheet can impart a marked hydrophilic feature to the material, allowing the solution to better permeate inside the film coating deposited on the surface. The careful rinsing of the sensor surface with water before the electrochemical detection allowed us to ensure that the signal is entirely due to the fraction of AA that was stably captured by the material. The improved performance of GO-Lys can be explained considering Lys capability to promote interactions with GLY and to improve the hydrophilicity of GO, as previously observed for other smart materials [58,59].

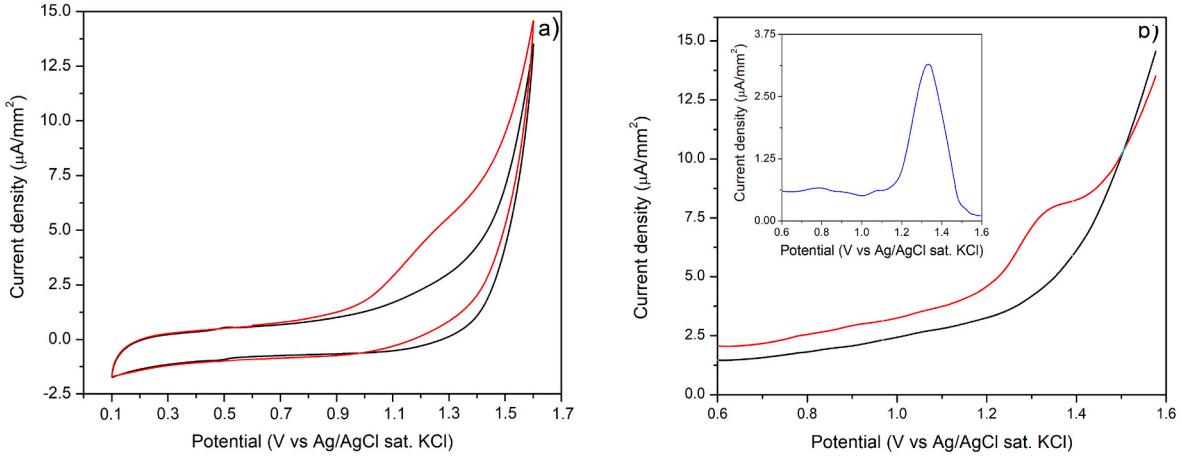

Fig. 5. a) CV and **b)** DPV responses collected with GO-Lys in a 0.1 M BR solution in absence (black lines) and in presence (red lines) of 20 mg/L GLY. The inset of **b** reports the response obtained for GLY oxidation after blank subtraction; the magnitudes in the x-y axes are the same of those reported in the main graph. (For interpretation of the references to colour in this figure legend, the reader is referred to the Web version of this article.)

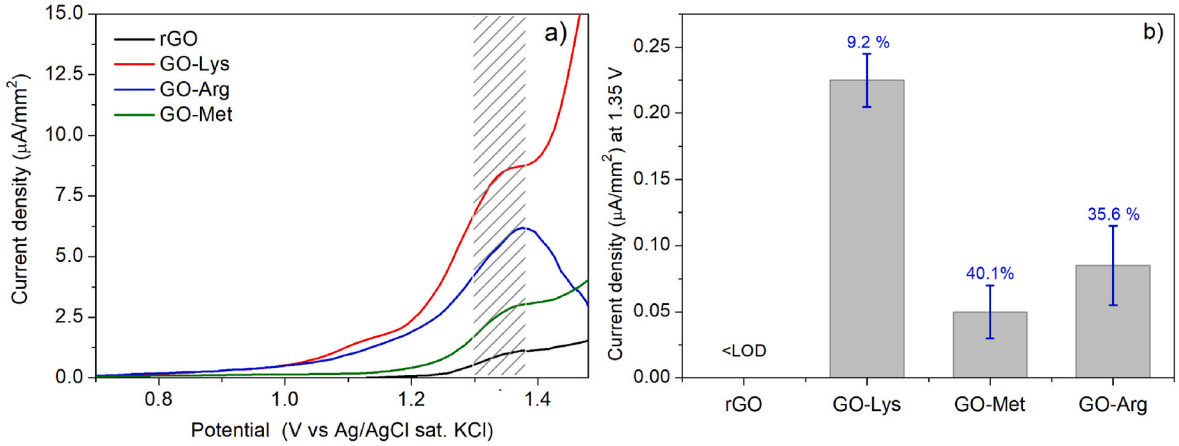

Fig. 6. a) DPV response recorded in 0.1 M BR (pH 6) after 15 min immersion of different modified electrodes in 10 mg/L GLY solution; **b)** mean current density values measured at +1.35 V and relative standard deviation obtained from three analyses performed in conditions like a), but after let in contact the coating with a GLY solution possessing a significantly lower concentration, namely 2 μg/L.

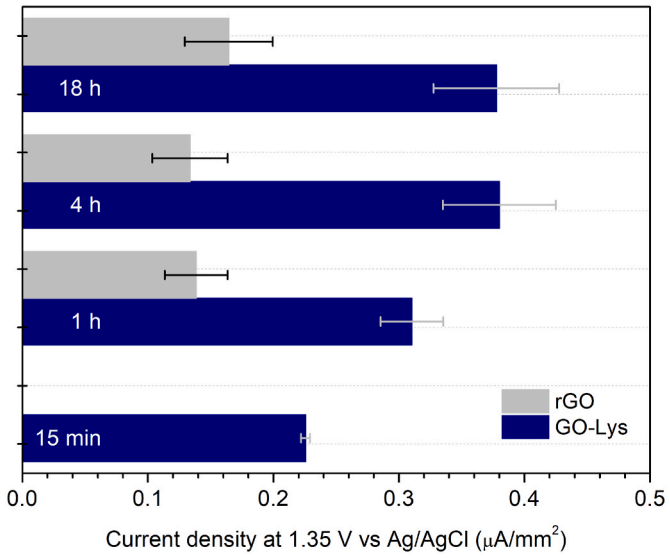

Fig. 7. Comparison of GO-Lys and rGO adsorption capacity towards GLY (2 μg/L solution) upon different incubation times (from 15 min up to 18 h). The average current values (I_p at +1.35 V) recorded at GO-Lys and rGO were extrapolated from DPV measurements. The experiments were performed in triplicate and the error bars describe the standard deviation. At a contact time of 15 min, no meaningful currents were recorded for rGO.

3.5. MD analysis the interaction between GLY and GO-AA

MD simulations were used to explain the improved performances for GLY capturing and detection of GO-AA compared to rGO. To shed light into the interaction of GLY with the different graphene sheets at atomistic level, the favourite adsorption sites of GLY on the surface of rGO and GO-AA were identified (Fig. 8a–d) and, through Molecular Mechanics-Generalized Born Surface Area (MM-GBSA) analysis, the binding energies were calculated (Fig. 8e).

The calculated binding affinities between GLY and GO-AA strongly increase when compared to rGO, in agreement with the electrochemical current values measured on the different modified electrodes after exposure to GLY. This suggest that GO-AA allows a better detection and oxidation of GLY due to stronger molecular interactions, which allow to capture the GLY molecules and stabilize them on the surface before oxidation. In particular, as observed from Fig. 8e, the values of the binding affinity of GLY for rGO, GO-Lys, GO-Met and GO-Arg perfectly reproduce the trend observed for the mean current values (Fig. 6b) measured with the different modified electrodes, highlighting the crucial role of the GLY capture step for its electrochemical detection.

MD simulations showed that in GO-AAs, GLY always interacts preferentially with the amino acid side chains grafted on the basal plane of GO. The binding affinity of GLY increases passing from rGO ($E_{binding} = -3.2$ kcal mol^{-1}) to GO-Met ($E_{binding} = -4.7$ kcal mol^{-1}) due to enhanced van der Waals interactions between GLY and Met side chain. The grafting of Arg and Lys causes the formation of "positively charged islands" on the GO, providing additional stabilizing electrostatic interactions with GLY, that is charged negatively. Specifically, the double negative phosphate group of GLY interacts with the side chains of Arg and Lys, installed on the GO, via multiple hydrogen bonds and salt bridges. Quite interestingly, Lys can interact better with GLY ($E_{binding} = -26.5$ kcal mol^{-1}) thanks to a highly localized positive charge, while in Arg the charge is delocalized over the entire Y-aromatic system of the guanidinium group ($E_{binding} = -8.6$ kcal mol^{-1}). In addition, Lys can "clamp" GLY better than Arg, because it can also interact with the carboxylic moiety of GLY, forming additional hydrogen bonds/salt bridge using its aminic moieties (Fig. 8f).

MD simulations allow us to conclude that the functionalization of GO with AA *i)* improves the affinity between GLY and the different nanosheets, increasing its capture *ii)* GO-Lys functionalization "clamps" GLY on the graphene surface, favouring its sensing.

3.6. Testing GO-Lys applicability in GLY sensing

GO-Lys was further tested in aqueous samples spiked with known concentration of GLY, ranging from 10 to 100 μg/L to assess the possibility to obtain a linear correlation between the signal and the concentration of analyte. In these tests, the sensor was simply dipped in the standard solution of the analyte and the signal was suddenly acquired, aiming at testing if GO-Lys can even rapidly detect GLY when its concentration in solution slightly increases. The samples containing GLY at various concentrations were first tested following a sequential order, going from the lowest to the highest concentration. The subtraction of the signal in the absence of analyte (Fig. 9a) once more evidenced the contribution of GLY oxidation, increasing in intensity at increasing the concentration of the analyte in solution, according to a linear correlation (see inset).

These same measurements were then repeated by testing solutions of GLY in the 2–100 μg/L concentration range in a randomized order, aiming at simulating the variability of the levels of pollutants in water matrices during the online monitoring system. The same electrode coating was used for all these measurements to evaluate the presence

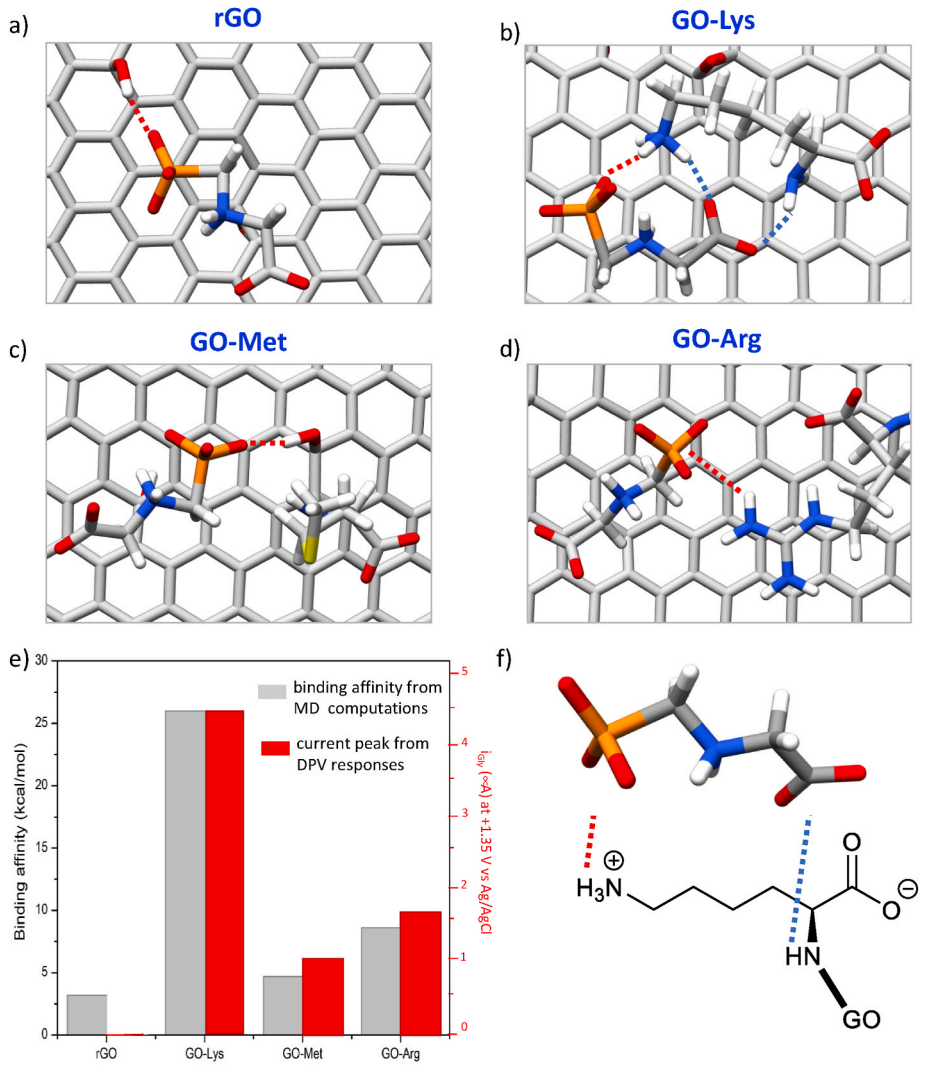

Fig. 8. Most interacting MD snapshots of GLY adsorption on a) rGO, b) GO-Lys, c) GO-Met and d) GO-Arg; the red dashed-line represents functional groups interacting with the phosphate moiety of the GLY, whereas the cyan dashed-line represents functional groups interacting with the carboxylic moiety of the GLY, as indicated in f) for the case of GLY with GO-Lys; e) bar graph representation of the binding affinity of GLY for rGO, GO-Lys, GO-Met and GO-Arg in relation with the average oxidation peak currents obtained with the same materials (see Fig. 6b). (For interpretation of the references to colour in this figure legend, the reader is referred to the Web version of this article.)

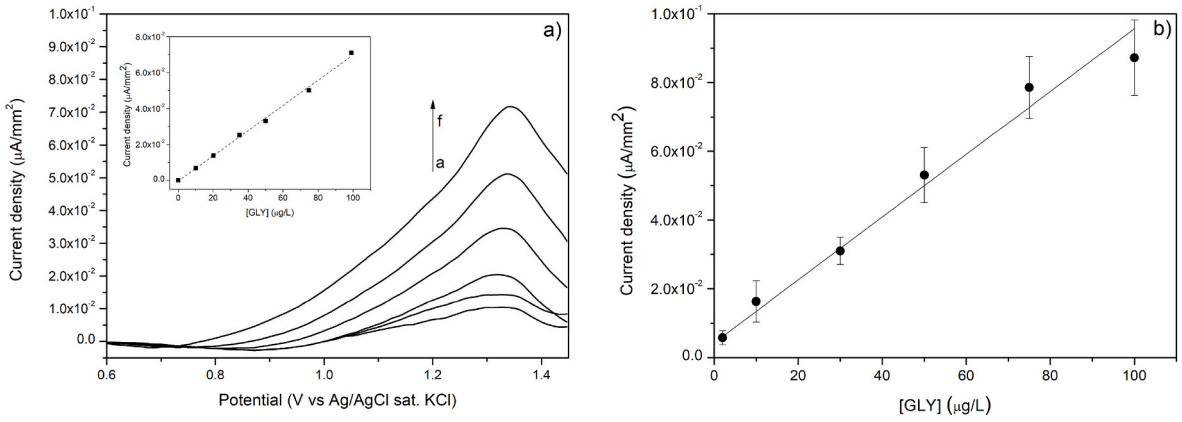

Fig. 9. a) DPV responses obtained, after blank subtraction, in 0.1 M BR solutions and GLY at increasing concentration from *a* to *f*, corresponding to 10, 20, 35, 50, 75, 100 mg/L **b)** Plot showing the correlation between the current peak and GLY concentration obtained by randomized analyses of the solution of GLY. The equation of resulting linear regression plot is $y = 0.91\ (\pm 0.04)\ 10^{-3}\ x + 0.43\ (\pm 0.11)\ 10^{-3}$, where the confidence limits for P = 95 % are included within arrows; $R^2 = 0.\ 9988$.

and, eventually, the impact of memory effects [60], which may affect the applicability of the device for the continuous monitoring of GLY in water. The response of the sensor in the pure electrolyte solution was acquired between the analysis of two solutions containing GLY, to highlight the possible accumulation of electroactive species on the sensor surface. These results (Fig. 9b) show that there is a linear correlation between the current recorded at +1.35 V and the concentration of analyte. Negligible memory effect was observed between consecutive measurements, as evidenced by the overlapping of signals recorded in the pure electrolyte solution after exposing the sensor to GLY and the response of the sensor showed quite a good repeatability, as testified by RSD ranging from 12 % for solutions at the highest concentrations to 35 % for solutions at the lowest ones. These results support the applicability of GO-Lys material as the sensing element of electrochemical devices for the continuous monitoring of GLY in water.

Although we decided not to proceed with a proper calculation of the limit of detection reachable by this sensor configuration, since our efforts are here directed to study the performance of the material specifically developed for such an application, it is worth to notice that we could obtain an answer significantly different from the blank signal even in solutions containing GLY at very low concentration, namely 2 μg/L. The concentration of GLY detectable can be further reduced by performing a pre-concentration step, i.e., letting the analyte in contact with the electrode coating, that are conditions naturally occurring in the water distribution network. This application requires to preliminary improve the mechanical stability of the sensing element, to avoid partial detachment from the underlaying electrode surface due to the pressure of the water flux; experiments in this direction are now in progress in our lab to obtain sensing cartridges based of GO-Lys.

4. Conclusions

In this work, we demonstrated the applicability of different GO-AAs for the electrochemical detection of GLY in aqueous media. Among the various GO derivatives tested, GO-Lys resulted the most performing material for the retention and subsequent electrochemical detection of GLY. The characterization of the materials at macroscopic and molecular levels allowed us to unveil the mechanism of detection, which is mainly attributed to the better ability of GO-Lys to interact with GLY molecules, stabilizing them on the surface and allowing a better charge transfer. Molecular modelling simulations suggested that the amino acid in L-Lys can clamp GLY molecules via hydrogen bonds and salt bridges. Due to this property and to the low charge transfer resistance characterizing GO-Lys, the material was used as the sensing element for the electrochemical detection of GLY. Preliminary electrochemical tests demonstrated that GO-Lys allowed the detection of this contaminant when present at a concentration as low as 2 μg/L. Further tests showed that the materials can be used for the realization of sensors possessing good linear response in a wide concentration range (up to 100 μg/L), good repeatability, negligible memory effects, and suitable for the detection of GLY in tap water. All these findings support the applicability of this material in the continuous monitoring of the contaminant in water. Once that GO-Lys has been included in a supporting matrix capable to improve the mechanical resistance of the sensing element to the hydrodynamic forces present in the water distribution line. Further experiments in this direction are in progress.

CRediT authorship contribution statement

Giulia Moro: Conceptualization, Formal analysis, Investigation, Writing – original draft. **Sara Khaliha:** Investigation. **Angela Pintus:** Investigation. **Sebastiano Mantovani:** Investigation. **Matteo Feltracco:** Investigation. **Andrea Gambaro:** Formal analysis. **Tainah D. Marforio:** Formal analysis. **Matteo Calvaresi:** Data curation, Methodology, Writing – review & editing. **Vincenzo Palermo:** Funding acquisition, Supervision, Writing – review & editing. **Manuela Melucci:** Conceptualization, Methodology, Project administration, Supervision, Writing – original draft. **Chiara Zanardi:** Conceptualization, Project administration, Supervision, Writing – original draft.

Declaration of competing interest

The authors declare the following financial interests/personal relationships which may be considered as potential competing interests: Manuela Melucci reports financial support was provided by European Union. Chiara Zanardi reports financial support was provided by Italian Ministry of Research. Manuela Melucci reports financial support was provided by Italian Ministry of Research. If there are other authors, they declare that they have no known competing financial interests or personal relationships that could have appeared to influence the work reported in this paper.

Data availability

Data will be made available on request.

Acknowledgment

The research leading to these results has received funding from the project 881603- GrapheneCore3-H2020-SGA-FET- SH1 Graphil-GRAPHENE-FLAGSHIP and from the European Union Next-GenerationEU - National Recovery and Resilience Plan (NRRP) – MISSION 4 COMPONENT 2of the “Interconnected Nord-Est Innovation Ecosystem” (iNEST - N. ECS00000043 - CUP N. H43C22000540006) and of the “Ecosystem for Sustainable Transition in Emilia-Romagna” (ECS_00000033_ECOSISTER).

Appendix A. Supplementary data

Supplementary data to this article can be found online at https://doi.org/10.1016/j.mtchem.2024.101936.

References

[1] S.D. Richardson, T.A. Ternes, Water analysis: emerging contaminants and current issues, Anal. Chem. 90 (2018) 473–505, https://doi.org/10.1021/acs.analchem.9b05269.
[2] C. Tsaridou, A.J. Karabelas, Drinking water standards and their implementation—a critical assessment, Water 13 (2021) 2918–2931, https://doi.org/10.3390/w13202918.
[3] M.J. Gunnarsdottir, S.M. Gardarsson, M.J. Figueras, C. Puigdomènech, R. Juárez, G. Saucedo, M.J. Arnedo, R. Santos, S. Monteiro, L. Avery, E. Pagaling, R. Allan, C. Abel, J. Eglitis, B. Hambsch, M. Hügler, A. Rajkovic, N. Smigic, B. Udovicki, H. J. Albrechtsen, A. López-Avilés, P. Hunter, Water safety plan enhancements with improved drinking water quality detection techniques, Sci. Total Environ. 698 (2020) 134185–134201, https://doi.org/10.1016/j.scitotenv.2019.134185.
[4] L. Schweitzer, J. Noblet, Water Contamination and Pollution, Elsevier, 2018, pp. 261–290, https://doi.org/10.1016/B978-0-12-809270-5.00011-X.
[5] https://sdgs.un.org/goals. (Accessed 12 July 2023).
[6] R. Meffe, I. de Bustamante, Emerging organic contaminants in surface water and groundwater: a first overview of the situation in Italy, Sci. Total Environ. 481 (2014) 280–295, https://doi.org/10.1016/j.scitotenv.2014.02.053.
[7] C.J. Houtman, Emerging contaminants in surface waters and their relevance for the production of drinking water in Europe, J. Integr. Environ. Sci. 7 (2010) 271–295, https://doi.org/10.1080/1943815X.2010.511648.
[8] K. Svensson, E. Tanner, C. Gennings, C. Lindh, H. Kiviranta, S. Wikström, C. G. Bornehag, Prenatal exposures to mixtures of endocrine disrupting chemicals and children’s weight trajectory up to age 5.5 in the SELMA study, Sci. Rep. 11 (2021) 11036–11051, https://doi.org/10.1038/s41598-021-89846-5.
[9] I. Yaroshenko, D. Kirsanov, M. Marjanovic, P.A. Lieberzeit, O. Korostynska, A. Mason, I. Frau, A. Legin, Real-Time water quality monitoring with chemical sensors, Sensors 20 (2020) 3432–3446, https://doi.org/10.3390/s20123432.
[10] H. Sohrabi, A. Hemmati, M.R. Majidi, S. Eyvazi, A. Jahanban-Esfahlan, B. Baradaran, R. Adlpour-Azar, A. Mokhtarzadeh, M. de la Guardia, Recent advances on portable sensing and biosensing assays applied for detection of main chemical and biological pollutant agents in water samples: a critical review, Trends Anal. Chem. 143 (2021) 116344–116356, https://doi.org/10.1016/j.trac.2021.116344.

[11] G. Moro, K. De Wael, L.M. Moretto, Challenges in the electrochemical (bio)sensing of nonelectroactive food and environmental contaminants, Curr. Opin. Electrochem. 16 (2019) 57–65, https://doi.org/10.1016/j.coelec.2019.04.019.
[12] B.I. Afghan, A.W. Wolkoff, High performance liquid chromatography in environmental analysis: present and future applications, J. Liq. Chromatogr. 4 (1981) 99–114, https://doi.org/10.1080/01483918108069353.
[13] S. Khizar, N. Zine, N. Jaffrezic-Renault, A. Elaissari, A. Errachid, Prospective analytical role of sensors for environmental screening and monitoring, Trends Anal. Chem. 157 (2022) 116751–116763, https://doi.org/10.1016/j.trac.2022.116751.
[14] R. Sivaranjanee, P. Senthil Kumar, R. Saravanan, M. Govarthanan, Electrochemical sensing system for the analysis of emerging contaminants in aquatic environment: a review, Chemosphere 294 (2022) 133779–133792, https://doi.org/10.1016/j.chemosphere.2022.133779.
[15] W. Jin, G. Maduraiveeran, Electrochemical detection of chemical pollutants based on gold nanomaterials, Trends Environ. Anal. Chem. 13 (2017) 10–25, https://doi.org/10.1016/j.teac.2017.05.001.
[16] G. Moro, H. Barich, K. Driesen, N.F. Montiel, L. Neven, C.D. Mendonça, Unlocking the full power of electrochemical fingerprinting for on-site sensing applications, Anal. Bioanal. Chem. 412 (2020) 5955–5971, https://doi.org/10.1007/s00216-020-02584-x.
[17] Y. Zuo, J. Xu, X. Zhu, X. Duan, L. Lu, Y. Yu, Graphene-derived nanomaterials as recognition elements for electrochemical determination of heavy metal ions: a review, Microchim. Acta 186 (2019) 171–184, https://doi.org/10.1007/s00604-019-3248-5.
[18] C.I.L. Justino, A.R. Gomes, A.C. Freitas, A.C. Duarte, T.A.P. Rocha-Santos, Graphene based sensors and biosensors, Trends Anal. Chem. 91 (2017) 53–71, https://doi.org/10.1016/j.trac.2017.04.003.
[19] W. Yang, K.R. Ratinac, S.R. Ringer, P. Thordarson, J.J. Gooding, F. Braet, Carbon nanomaterials in biosensors: should you use nanotubes or graphene? Angew. Chem. Int. Ed. 49 (2010) 2114–2131, https://doi.org/10.1002/anie.200903463.
[20] A.D. da Silva, W.J. Paschoalino, J.P.V. Damasceno, L.T. Kubota, Structure, properties, and electrochemical sensing applications of graphene-based materials, Chemelectrochem 7 (2020) 4508–4521, https://doi.org/10.1002/celc.202001168.
[21] F. Vulcano, A. Kovtun, C. Bettini, Z. Xia, A. Liscio, A. Terzi, A. Heras, A. Colina, B. Zanfrognini, M. Melucci, V. Palermo, C. Zanardi, Dopamine-functionalized graphene oxide as a high-performance material for biosensing, 2D Mater. 7 (2020) 24007–24016, https://doi.org/10.1088/2053-1583/ab734f.
[22] F. Poletti, B. Zanfrognini, L. Favaretto, V. Quintano, J. Sun, E. Treossi, M. Melucci, V. Palermo, C. Zanardi, Continuous capillary-flow sensing of glucose and lactate in sweat with an electrochemical sensor based on functionalized graphene oxide, Sensor. Actuator. B 344 (2021) 130253–130271, https://doi.org/10.1016/j.snb.2021.130253.
[23] A. Silvestri, A. Criado, F. Poletti, F. Wang, P. Fanjul-Bolado, M.B. González-García, C. García-Astrain, L.M. Liz-Marzán, X. Feng, C. Zanardi, M. Prato, Bio-responsive, electroactive and inkjet-printable graphene-based inks, Adv. Funct. Mater. 32 (2022) 2105028–2105036, https://doi.org/10.1002/adfm.202105028.
[24] S. Khaliha, A. Bianchi, A. Kovtun, F. Tunioli, A. Boschi, M. Zambianchi, D. Paci, L. Bocchi, S. Valsecchi, S. Polesello, A. Liscio, M. Bergamini, M. Brunetti, M. L. Navacchia, V. Palermo, M. Melucci, Graphene oxide nanosheets for drinking water purification by tandem adsorption and microfiltration, Sep. Purif. Technol. 300 (2022) 121826–121834, https://doi.org/10.1016/j.seppur.2022.121826.
[25] S. Khaliha, T.D. Marforio, A. Kovtun, S. Mantovani, A. Bianchi, M.L. Navacchia, M. Zambianchi, L. Bocchi, N. Boulanger, A. Iakunkov, M. Calvaresi, A.V. Talyzin, V. Palermo, M. Melucci, Defective graphene nanosheets for drinking water purification: adsorption mechanism, performance, and recovery, FlatChem 29 (2021) 100283–100297, https://doi.org/10.1016/j.flatc.2021.100283.
[26] S. Mantovani, S. Khaliha, L. Favaretto, A. Bettini, A. Kovtun, M. Zambianchi, M. Gazzano, B. Casentini, V. Palermo, M. Melucci, Scalable synthesis and purification of functionalized graphene nanosheets for water remediation, Chem. Commun. 57 (2021) 3765–3791, https://doi.org/10.1039/D1CC00704A.
[27] S. Mantovani, S. Khaliha, T.D. Marforio, A. Kovtun, L. Favaretto, F. Tunioli, A. Bianchi, G. Petrone, A. Liscio, V. Palermo, M. Calvaresi, M.L. Navacchia, M. Melucci, Facile high-yield synthesis and purification of lysine-modified graphene oxide for enhanced drinking water purification, Chem. Commun. 58 (2022) 9766–9780, https://doi.org/10.1039/D2CC03256B.
[28] S. Mantovani, T.D. Marforio, S. Khaliha, A. Pintus, A. Kovtun, F. Tunioli, L. Favaretto, A. Bianchi, M.L. Navacchia, V. Palermo, M. Calvaresi, M. Melucci, Amino acid-driven adsorption of emerging contaminants in water by modified graphene oxide nanosheets, Environ. Sci.: Water Res. Technol. 9 (2023) 1030–1042, https://doi.org/10.1039/D2EW00871H.
[29] A. Pintus, S. Mantovani, A. Kovtun, G. Bertuzzi, M. Melucci, M. Bandini, Recyclable GO-arginine hybrids for CO_2 fixation into cyclic carbonates, Chem. Eur J. 29 (2023) e202202440, https://doi.org/10.1002/chem.202202440.
[30] W. Zhou, W. Zhuang, L. Ge, Z. Wang, J. Wu, H. Niu, D. Liu, C. Zhu, Y. Chen, H. Ying, Surface functionalization of graphene oxide by amino acids for *Thermomyces lanuginosus* lipase adsorption, J. Colloid Interface Sci. 546 (2019) 211–224, https://doi.org/10.1016/j.jcis.2019.03.066.
[31] Y. Liang, J. Luo, D. Milstein, Facile synthesis of amides *via* acceptorless dehydrogenative coupling of aryl epoxides and amines, Chem. Sci. 13 (2022) 5913–5925, https://doi.org/10.1039/D2SC01959K.
[32] V. Silva, L. Montanarella, A. Jones, O. Fernández-Ugalde, H.G.J. Mol, C.J. Ritsema, V. Geissen, Distribution of glyphosate and aminomethylphosphonic acid (AMPA) in agricultural topsoils of the European Union, Sci. Total Environ. 621 (2018) 1352–1371, https://doi.org/10.1016/j.scitotenv.2017.10.093.
[33] I. Heap, S.O. Duke, Overview of glyphosate-resistant weeds worldwide, Pest Manag. Sci. 74 (2018) 1040–1052, https://doi.org/10.1002/ps.4760.
[34] C.M. Benbrook, Trends in glyphosate herbicide use in the United States and globally, Environ. Sci. Eur. 28 (2023) 3–15, https://doi.org/10.1186/s12302-016-0070-0.
[35] Y. Yang, X. Zhang, J. Jiang, J. Han, W. Li, X. Li, K. Mei, Y. Leung, S.A. Snyder, P.J. J. Alvarez, Which micropollutants in water environments deserve more attention globally? Environ. Sci. Technol. 56 (2022) 1–13, https://doi.org/10.1021/acs.est.1c04250.
[36] T.R.T. Santos, M.B. Andrade, M.F. Silva, R. Bergamasco, S. Hamoudi, Development of α- and γ-Fe_2O_3 decorated graphene oxides for glyphosate removal from water, Environ. Technol. 40 (2019) 1118–1126, https://doi.org/10.1080/09593330.2017.1411397.
[37] D. Grau, N. Grau, Q. Gascuel, C. Paroissin, C. Stratonovitch, D. Lairon, D. A. Devault, J. Di Cristofaro, Quantifiable urine glyphosate levels detected in 99% of the French population, with higher values in men, in younger people, and in farmers, Environ. Sci. Pollut. Res. 29 (2022) 32882–32895, https://doi.org/10.1007/s11356-021-18110-0.
[38] J.O. Ighalo, O.J. Ajala, A.G. Adeniyi, E.O. Babatunde, M.A. Ajala, Ecotoxicology of glyphosate and recent advances in its mitigation by adsorption, Environ. Sci. Pollut. Res. 28 (2021) 2655–2670, https://doi.org/10.1007/s11356-020-11521-5.
[39] M. Feltracco, E. Barbaro, E. Morabito, R. Zangrando, R. Piazza, C. Barbante, A. Gambaro, Assessing glyphosate in water, marine particulate matter, and sediments in the lagoon of Venice, Environ. Sci. Pollut. Res. 29 (2022) 16383–16397, https://doi.org/10.1007/s11356-021-16957-x.
[40] S.H. Bai, S.M. Ogbourne, Glyphosate: environmental contamination, toxicity and potential risks to human health via food contamination, Environ. Sci. Pollut. Res. 23 (2016) 18988–18998, https://doi.org/10.1007/s11356-016-7425-3.
[41] S. Krimsky, Glyphosate-based herbicides and public health: making sense of the science, J. Agric. Environ. Ethics 35 (2021) 3–24, https://doi.org/10.1007/s10806-021-09874-z.
[42] A.L. Valle, F.C.C. Mello, R.P. Alves-Balvedi, L.P. Rodriguez, L.R. Goulart, Glyphosate detection: methods, needs and challenges, Environ. Chem. Lett. 17 (2019) 291–306, https://doi.org/10.1007/s10311-018-0789-5.
[43] L.A. Zambrano-Intriago, C.G. Amorim, J.M. Rodríguez-Díaz, A.N. Araújo, M. Montenegro, Challenges in the design of electrochemical sensor for glyphosate-based on new materials and biological recognition, Sci. Total Environ. 793 (2021) 148496–148506, https://doi.org/10.1016/j.scitotenv.2021.148496.
[44] J.S. Noori, J. Mortensen, A. Geto, Recent development on the electrochemical detection of selected pesticides: a focused review, Sensors 20 (2020) 2221–2241, https://doi.org/10.3390/s20082221.
[45] C.T. Thanh, N.H. Binh, P.N.D. Duoc, V.T. Thu, P.V. Trinh, N.N. Anh, N.V. Tu, N. V. Tuyen, N.V. Quynh, V.C. Tu, B.T.P. Thao, P.D. Thang, H. Abe, N.V. Chuc, Electrochemical sensor based on reduced graphene oxide/double-walled carbon nanotubes/octahedral Fe_3O_4/chitosan composite for glyphosate detection, Bull. Environ. Contam. Toxicol. 106 (2021) 1017–1024, https://doi.org/10.1007/s00128-021-03179-7.
[46] S.L. Cahuantzi-Muñoz, M.A. González-Fuentes, L.A. Ortiz-Frade, E. Torres, S. Ţălu, G. Trejo, A. Méndez-Albores, Electrochemical biosensor for sensitive quantification of glyphosate in maize kernels, Electroanalysis 31 (2022) 927–1007, https://doi.org/10.1002/elan.201800759.
[47] V. Caratelli, G. Fegatelli, D. Moscone, F. Arduini, A paper-based electrochemical device for the detection of pesticides in aerosol phase inspired by nature: a flower-like origami biosensor for precision agriculture, Biosens. Bioelectron. 205 (2022) 114119–114127, https://doi.org/10.1016/j.bios.2022.114119.
[48] S. Thimoonnee, K. Somnet, P. Ngaosri, S. Chairam, C. Karuwan, W. Kamsong, A. Tuantranont, M. Amatatongchai, Fast, Sensitive and selective simultaneous determination of paraquat and glyphosate herbicides in water samples using a compact electrochemical sensor, Anal. Methods 14 (2022) 820–832, https://doi.org/10.1039/D1AY02201F.
[49] J.S. Santos, M.S. Pontes, E.F. Santiago, A.R. Fiorucci, G.J. Arruda, An efficient and simple method using a graphite oxide electrochemical sensor for the determination of glyphosate in environmental samples, Sci. Total Environ. 749 (2020) 142385–142397, https://doi.org/10.1016/j.scitotenv.2020.142385.
[50] D. Liu, Z. Shao, J. Gui, M. Chen, M. Liu, G. Cui, S. Pang, Y. Zhou, A polar-hydrophobic ionic liquid induces grain growth and stabilization in halide perovskites, Chem. Commun. 55 (2019) 11059–11072, https://doi.org/10.1039/C9CC05490A.
[51] G. Maccaferri, C. Zanardi, Z.Y. Xia, A. Kovtun, A. Liscio, F. Terzi, V. Palermo, R. Seeber, Systematic study of the correlation between surface chemistry, conductivity and electrocatalytic properties of graphene oxide nanosheets, Carbon 120 (2017) 165–182, https://doi.org/10.1016/j.carbon.2017.05.030.
[52] F. Poletti, A. Scida, B. Zanfrognini, A. Kovtun, V. Parkula, L. Favaretto, M. Melucci, V. Palermo, E. Treossi, C. Zanardi, Graphene-paper-based electrodes on plastic and textile supports as new platforms for amperometric biosensing, Adv. Funct. Mater. 32 (2022) 2107941–2107953, https://doi.org/10.1002/adfm.202107941.
[53] J. Wang, R.M. Wolf, J.W. Caldwell, P.A. Kollman, D.A. Case, Development and testing of a general amber force field, J. Comput. Chem. 25 (2004) 1157–1165, https://doi.org/10.1002/jcc.20035.
[54] C.I. Bayly, P. Cieplak, W. Cornell, P.A. Kollman, A well-behaved electrostatic potential based method using charge restraints for deriving atomic charges: the RESP Model, J. Phys. Chem. 97 (1993) 10269–10278, https://doi.org/10.1021/j100142a004.
[55] B.R.I.I.I. Miller, T.D.J. McGee, J.M. Swails, N. Homeyer, H. Gohlke, A.E. Roitberg, A.E. Mmpbsa, py: an efficient program for end-state free energy calculations,

J. Chem. Theor. Comput. 8 (2012) 3314–3331, https://doi.org/10.1021/ct300418h.
[56] A. Ambrosi, C.K. Chua, A. Bonanni, M. Pumera, Electrochemistry of graphene and related materials, Chem. Rev. 114 (2014) 7150–7188, https://doi.org/10.1021/cr500023c.
[57] F. Poletti, L. Favaretto, A. Kovtun, E. Treossi, F. Corticelli, M. Gazzano, V. Palermo, C. Zanardi, M. Melucci, Electrochemical sensing of glucose by chitosan modified graphene oxide, J. Phys. Mater. 3 (2020) 14011–14036, https://doi.org/10.1088/2515-7639/ab5e51.
[58] Z.H. Liu, Q.M. Wang, Q.F. Lü, J. Wu, L-lysine functionalized $Ti_3C_2T_x$ coated polyurethane sponge for high-throughput oil–water separation, Colloids Surf., A 640 (2022) 128396–128405, https://doi.org/10.1016/j.colsurfa.2022.128396.
[59] J. Wang, J. Wang, S. Qiu, W. Chen, L. Cheng, W. Du, J. Wang, L. Han, L. Song, Y. Hu, Biodegradable L-lysine-modified amino black phosphorus/poly(L-lactide-Coε-Caprolactone) nanofibers with enhancements in hydrophilicity, shape recovery and osteodifferentiation properties, Colloids Surf., B 209 (2022) 112209–112219, https://doi.org/10.1016/j.colsurfb.2021.112209.
[60] C.M.A. Brett, Electrochemical sensors for environmental monitoring. strategy and examples, Pure Appl. Chem. 73 (2001) 1969–1979, https://doi.org/10.1351/pac200173121969.